Electronic Supplementary Material (ESI) for Inorganic Chemistry Frontiers.

Supporting Information

$CaCe(IO_3)_3(IO_3F)F$: A Promising Nonlinear Optical Material Containing both IO_3^- and IO_3F^{2-} Anions

Nan Ma,[abc] Chun-Li Hu,[c] Jin Chen,[c] Zhi Fang,[c] Yu Huang,[c] Bing-Xuan Li,[c] and Jiang-Gao Mao*[abc]

[a] Faculty of Materials Metallurgy and Chemistry, Jiangxi University of Science and Technology, Ganzhou 341000, People's Republic of China.

[b] Ganjiang Innovation Academy, Chinese Academy of Sciences, Ganzhou 341119, People's Republic of China.

[c] State Key Laboratory of Structural Chemistry, Fujian Institute of Research on the Structure of Matter, Chinese Academy of Sciences, Fuzhou 350002, P. R. China.

* Corresponding Authors: mjg@fjirsm.ac.cn

Table of Contents

Table S1. Space groups and SHG effects of the cerium iodates reported.

	Compound	Space group	SHG	Ref
Ce (III)	$Ce(IO_3)_3$	$P2_1/a$	N/A	1
	$Ce(VO_3)_2(IO_3)$	*Pbcm*	N/A	2
	$NaCe(IO_3)_4$	*Cc*	50 × α - SiO_2	3
	$Ce(MoO_2)(IO_3)_4(OH)$	$P2_1$	negligible	4
	$Ce_3Pb_3(IO_3)_{13}O$	$R3c$	very weak	5
	$Ce_2I_6O_{18}$	$P2_1$	9 × KDP	6
Ce(IV)	$Ce(IO_3)_4{\cdot}H_2O$	$P2_1/n$	N/A	7
	$Ce(IO_3)_4$	$R3c$	0.9 × KDP	8
	$Ce_2(IO_3)_8(H_2O)$	$R3c$	1.3 × KDP	9
	$Ce(IO_3)_2F_2{\cdot}H_2O$	$Ima2$	~ 3 × KDP	10
	$Ce_2(IO_3)_6(O)$	*Pnma*	N/A	11
	$K_8Ce_2I_{18}O_{53}$	$C2/c$	N/A	12
	$Li_2Ce(IO_3)_4F_2$	$C2/c$	N/A	13
	$Ce(IO_3)_2(SO_4)$	$P2_12_12_1$	3.5 × KDP	14
	$CeCu(IO_3)_5$	$Pna2_1$	N/A	15
	$Ce(IO_3)_2F_2$	$Pna2_1$	5.5 × KDP	16
Intermediate-valence Ce (III)/ Ce(IV)	$Ce_2(IO_3)_6(OH_{0.44})$	*Pnma*	N/A	11
	$K_3Ce_9(IO_3)_{36}$	$R3c$	0.4 × KDP	17
	$La_{0.3}Ce_9(IO_3)_{36}$	$R3c$	1.1 × KDP	17

Table S2. Crystallographic data for $CaCe(IO_3)_3(IO_3F)F$.

Formula	$CaCe(IO_3)_3(IO_3F)F$
Formula weight	917.80
Temperature/K	293.5(1)
Crystal system	orthorhombic
Space group	$Pna2_1$
a/Å	11.0676(10)
b/Å	18.1507(15)
c/Å	6.0301(6)
Volume/Å^3	1211.35(19)
Z	4
ρ_{calc}g/cm^3	5.033
μ/mm^{-1}	14.464
F(000)	1616.0
Radiation	MoKα(λ= 0.71073)
Independent reflections	2875 [R_{int} = 0.0556, R_{sigma} = 0.0586]
Goodness-of-fit on F^2	1.042
Final R indexes [I>=2σ (I)]	R_1 = 0.0361, wR_2 = 0.0716
Final R indexes [all data]	R_1 = 0.0455, wR_2 = 0.0765
Flack parameter	0.02(3)

$^aR_1 = \sum||F_o| - |F_c||/\sum|F_o|$, and $wR_2 = \{\sum w[(F_o)^2 - (F_c)^2]^2/\sum w[(F_o)^2]^2\}^{1/2}$.

Table S3. Selected Bond Lengths for $CaCe(IO_3)_3(IO_3F)F$.

Atom	Length/Å	Atom	Length/Å
Ce(1)- O(1)	2.343(9)	I(1)- O(2)	1.799(9)
Ce(1)- O(3)	2.585(8)	I(1)- O(3)	1.851(10)
Ce(1)- O(4)	2.288(9)	I(2)- O(4)	1.816(9)
Ce(1)- O(8)#1	2.305(10)	I(2)- O(5)	1.811(9)
Ce(1)- O(9)	2.128(9)	I(2)- O(6)	1.795(10)
Ce(1)- O(12)	2.429(8)	I(3A)- O(7)	1.821(8)
Ce(1)- F(1)#2	2.260(9)	I(3A)- O(8)	1.839(12)
Ce(1)- F(2)	2.283(8)	I(3A)- O(9)	1.902(10)
Ca(1)- O(2)#3	2.448(10)	I(3A)- F(1)	2.457(9)
Ca(1)- O(3)#4	2.376(9)	I(3B)- O(7)	1.810(8)
Ca(1)- O(5)#5	2.780(10)	I(3B)- O(8)	1.780(11)
Ca(1)- O(7)#4	2.366(11)	I(3B)- O(9)	2.450(10)
Ca(1)- O(10)#6	2.368(10)	I(3B)- F(1)	1.914(9)
Ca(1)- O(11)	2.358(10)	I(4)- O(10)	1.811(10)
Ca(1)- F(2)	2.288(8)	I(4)- O(11)	1.811(9)
I(1)- O(1)	1.833(9)	I(4)- O(12)	1.815(10)

Symmetry transformations for the atoms generated: #1 x, y, -1+z; #2 -1/2+x, 3/2-y, -1+z; #3 1/2-x, -1/2+y, 1/2+z; #4 -1/2+x, 3/2-y, +z; #5 1/2-x, -1/2+y, -1/2+z; #6 1-x, 1-y, 1/2+z.

Table S4. Calculated dipole moments of IO_3, IO_3F, CeO_6F_2 and CaO_6F units, and net dipole moment of a unit cell for $CaCe(IO_3)_3(IO_3F)F$.

$CaCe(IO_3)_3(IO_3F)F$				
NCS unit (a unit cell)	**Dipole moment (D)**			
	***x*-component**	**y-component**	***z*-component**	**total magnitude**
$I(1)O_3$	±8.1038	±6.75735	11.36242	15.50606
$I(2)O_3$	±7.421973	±7.30217	11.43305	15.46357
$I(3)O_3$	±6.61056	±6.648737	5.398055	10.8187
$I(4)O_3$	±0.44606	±5.38661	14.68387	15.64706
$Ce(1)O_6F_2$	±0.950878	±0.80821	-0.46352	1.331253
$Ca(1)O_6F$	±1.82597	±1.90877	-0.37958	2.668645
Net dipole moment	0	0	168.1372	168.1372
Cell Volume/$Å^3$	1211.35			
The dipole moment density (D/$Å^3$)	0.138801			

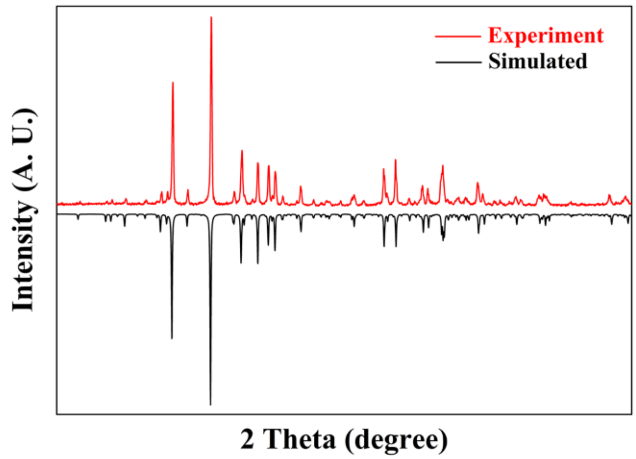

Fig. S1. Simulated and measured PXRD patterns of $CaCe(IO_3)_3(IO_3F)F$.

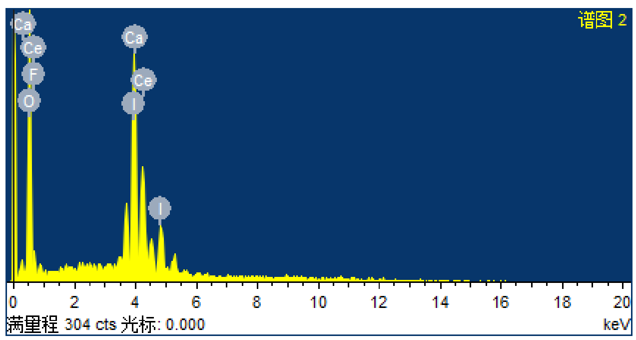

Fig. S2. The EDS analysis of $CaCe(IO_3)_3(IO_3F)F$.

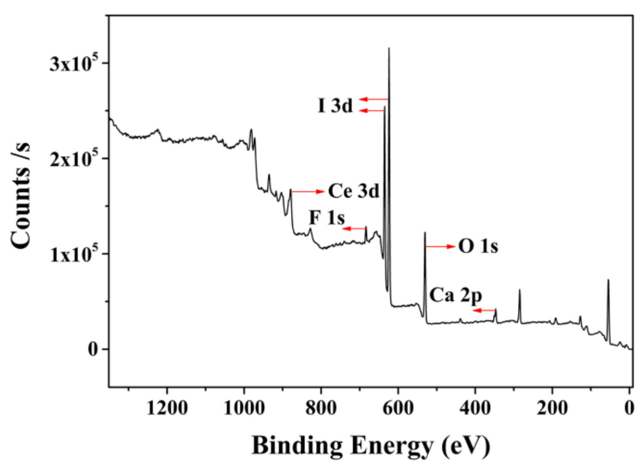

Fig. S3. XPS spectrum of $CaCe(IO_3)_3(IO_3F)F$.

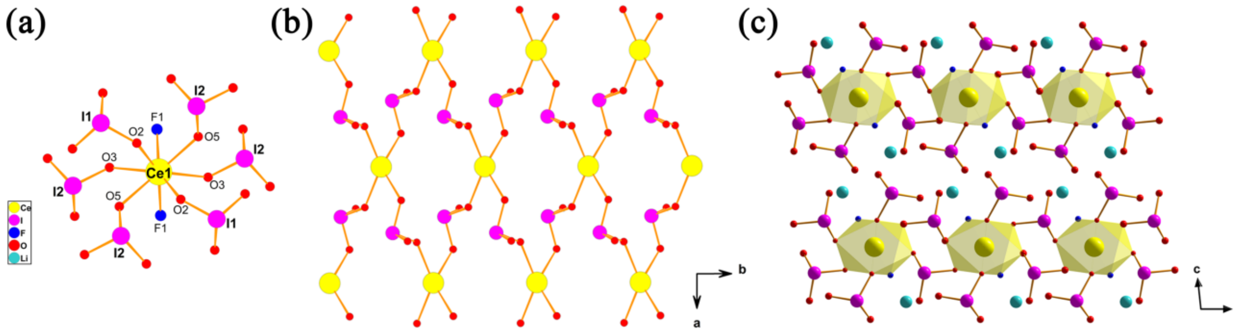

Fig. S4 The coordination geometry of the Ce^{4+} cation in $Li_2Ce(IO_3)_4F_2$ (a), a 2D $[Ce(IO_3)_2]^{2+}$ layer parallels to the ab plane in $Li_2Ce(IO_3)_4F_2$ (b), view of the structure of $Li_2Ce(IO_3)_4F_2$ down the $b-$ axis (c).

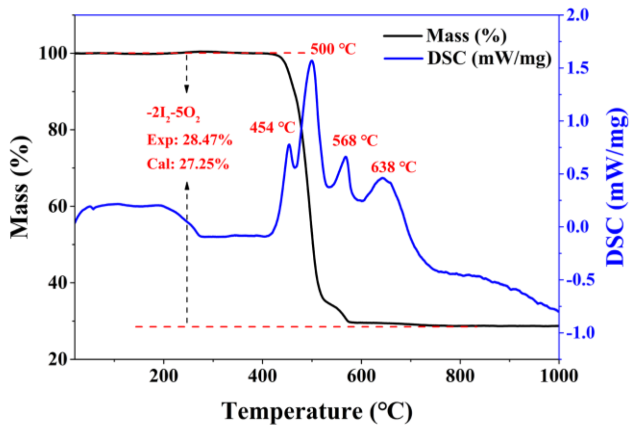

Fig. S5. TGA and DSC curves of $CaCe(IO_3)_3(IO_3F)F$ under a N_2 atmosphere.

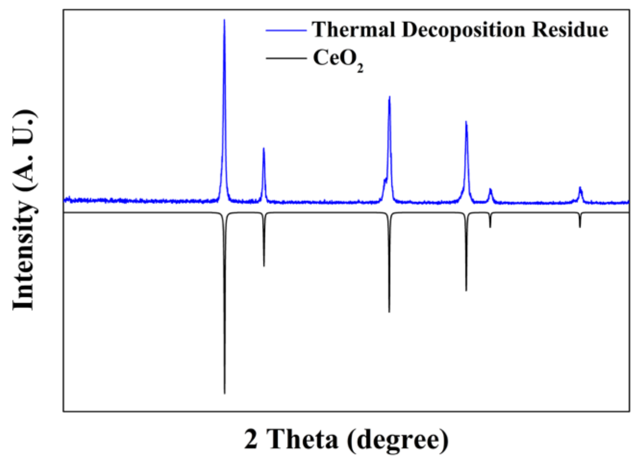

Fig. S6. Comparison of the powder XRD patterns of the thermal decomposition residues and CeO_2 standard

Reference

1 X. A. Chen, L. Zhang, X. A. Chang, H. G. Zang and W. Q. Xiao, Cerium triiodate, $Ce(IO_3)_3$, *Acta Crystallogr., Sect. C: Cryst. Struct. Commun.*, 2005, **61**, I61-I62.

2 T. Eaton, J. Lin, J. N. Cross, J. T. Stritzinger and T. E. Albrecht-Schmitt, $Th(VO_3)_2(SeO_3)$ and $Ln(VO_3)_2(IO_3)$ (Ln = Ce, Pr, Nd, Sm, and Eu): unusual cases of aliovalent substitution, *Chem. Commun.*, 2014, **50**, 3668-3670.

3 S. J. Oh, H. G. Kim, H. Jo, T. G. Lim, J. S. Yoo and K. M. Ok, Photoconversion Mechanisms and the Origin of Second-Harmonic Generation in Metal Iodates with Wide Transparency, $NaLn(IO_3)_4$ (Ln = La, Ce, Sm, and Eu) and $NaLa(IO_3)_4$: Ln^{3+} (Ln = Sm and Eu), *Inorg. Chem.*, 2017, **56**, 6973-6981.

4 J. Lin, Q. Liu, Z. H. Yue, K. Diefenbach, L. W. Cheng, Y. J. Lin and J. Q. Wang, Expansion of the structural diversity of f-element bearing molybdate iodates: synthesis, structures, and optical properties, *Dalton Trans.*, 2019, **48**, 4823-4829.

5 T. Hu, L. Qin, F. Kong, Y. Zhou and J. G. Mao, $Ln_3Pb_3(IO_3)_{13}(\mu^3{-}O)$ (Ln = La−Nd): New Types of Second-Order Nonlinear Optical Materials Containing Two Types of Lone Pair Cations, *Inorg. Chem.*, 2009, **48**, 2193-2199.

6 L. Xiao, Z. B. Cao, J. Y. Yao, Z. S. Lin and Z. G. Hu, A new cerium iodate infrared nonlinear optical material with a large second-harmonic generation response, *J. Mater. Chem. C*, 2017, **5**, 2130-2134.

7 J. A. Ibers, The Crystal Structure of Ceric Iodate Monohydrate, *Acta Cryst.*, 1956, **9**, 225-231.

8 T. H. Wu, X. X. Jiang, C. Wu, H. Y. Sha, Z. J. Wang, Z. S. Lin, Z. P. Huang, X. F. Long, M. G. Humphrey and C. Zhang, From $Ce(IO_3)_4$ to $CeF_2(IO_3)_2$: fluorinated homovalent substitution simultaneously enhances SHG response and bandgap for mid-infrared nonlinear optics, *J. Mater. Chem. C*, 2021, **9**, 8987-8993.

9 Y. X. Wang, T. Duan, Z. H. Weng, J. Ling, X. M. Yin, L. H. Chen, D. P. Sheng, J. Diwu, Z. F. Chai, N. Liu and S. A. Wang, Mild Periodic Acid Flux and Hydrothermal Methods for the Synthesis of Crystalline f-Element-Bearing Iodate Compounds, *Inorg. Chem.*, 2017, **56**, 13041-13050.

10 T. Abudouwufu, M. Zhang, S. C. Cheng, Z. H. Yang and S. L. Pan, $Ce(IO_3)_2F_2{\cdot}H_2O$: The First Rare-Earth-Metal Iodate Fluoride with Large Second Harmonic Generation Response, *Chem. Eur. J.*, 2019, **25**, 1221-1226.

11 R. E. Sykora, L. Deakin, A. Mar, S. Skanthakumar, L. Soderholm and T. E. Albrecht-Schmitt, Isolation of Intermediate-valent Ce(III)/Ce(IV) Hydrolysis Products in the Preparation of Cerium Iodates: Electronic and Structural Aspects of $Ce_2(IO_3)_6(OH_x)$($x \approx 0$ and 0.44), *Chem. Mater.*, 2004, **16**, 1343-1349.

12 R. F. Wu, X. X. Jiang, M. J. Xia, L. J. Liu, X. Y. Wang, Z. S. Lin and C. T. Chen, $K_8Ce_2I_{18}O_{53}$: a novel potassium cerium(IV) iodate with enhanced visible light driven photocatalytic activity resulting from polar zero dimensional $[Ce(IO_3)_8]^{4-}$ units, *Dalton Trans.*, 2017, **46**, 4170-4173.

13 C. C. Tang, X. X. Jiang, S. Guo, R. X. Guo, L. J. Liu, M. J. Xia, Q. Huang, Z. S. Lin and X. Y. Wang, Synthesis, Crystal Structure, and Optical Properties of the First Alkali Metal Rare-Earth Iodate Fluoride: $Li_2Ce(IO_3)_4F_2$, *Cryst. Growth Des.*, 2020, **20**, 2135-2140.
14 T. H. Wu, X. X. Jiang, Y. R. Zhang, Z. J. Wang, H. Y. Sha, C. Wu, Z. S. Lin, Z. P. Huang, X. F. Long, M. G. Humphrey and C. Zhang, From $CeF_2(SO_4)\cdot H_2O$ to $Ce(IO_3)_2(SO_4)$: Defluorinated Homovalent Substitution for Strong Second-Harmonic-Generation Effect and Sufficient Birefringence, *Chem. Mater.*, 2021, **33**, 9317-9325.
15 L. Geng, C. Y. Meng and Q. Yan, Polar lanthanide copper iodates $LnCu(IO_3)_5$ (Ln = La, Ce, Pr, and Nd): Synthesis, crystal structure and characterization, *J. Solid State Chem.*, 2022, **308**, 122934.
16 X. H. Zhang, B. P. Yang, C. L. Hu, J. Chen, Q. M. Huang and J. G. Mao, A New Anhydrous Polar Rare-Earth Iodate Fluoride, $Ce(IO_3)_2F_2$, Exhibiting a Large Second-Harmonic-Generation Effect and Improved Overall Performance, *Chem. Mater.*, 2021, **33**, 2894-2900.
17 H. X. Tang, C. Zhuo, Y. X. Zhang, Q. R. Shui, R. B. Fu, Z. J. Ma and X. T. Wu, $A_xCe_9(IO_3)_{36}$ (A = K, La): the effects of a change in the intermediate valence on the second-harmonic generation response, *Dalton Trans.*, 2020, **49**, 3672-3675.